World Academy of Science, Engineering and Technology
International Journal of Electronics and Communication Engineering
Vol:10, No:2, 2016

Modeling and Simulation of Practical Metamaterial Structures

Ridha Salhi, Mondher Labidi, Fethi Choubani

***Abstract*—**Metamaterials have attracted much attention in recent years because of their electromagnetic exquisite proprieties. We will present, in this paper, the modeling of three metamaterial structures by equivalent circuit model. We begin by modeling the SRR (Split Ring Resonator), then we model the HIS (High Impedance Surfaces), and finally, we present the model of the CPW (Coplanar Wave Guide). In order to validate models, we compare the results obtained by an equivalent circuit models with numerical simulation.

***Keywords*—**Metamaterials, SRR, HIS, CPW, IDC.

I. Introduction

METAMATERIALS are artificial materials engineered to have properties that have not yet been found in nature. The most interesting feature is the ability to control or modify the permittivity and permeability of the material to obtain a behavior adapted to a specific application.

Metamaterials are used to improve the performance of the antennas, filters, and couplers. Their main advantage is the miniaturization of devices due to a refractive index that can easily be adjusted or even negative at certain frequencies [1]. Indeed, the value of the refractive index becomes negative when the permittivity and the permeability of the material are simultaneously negative.

In general, the metamaterials are manufactured from metal inclusions embedded in a dielectric substrate. The interaction of electromagnetic fields with inclusions produces the typical resonant behavior that characterizes metamaterials.

The magnetic field induces a current in the metal ring producing an inductive effect. A capacitive effect appears between the metal parts placed at different potential [2].

We focus in this paper to present the equivalent circuit models of three metamaterial structures. We begin by modeling the SRR (Split Ring Resonator), then we model the HIS (High Impedance Surfaces), and finally, we present the model of the CPW (Coplanar Wave Guide). Each time, we compare the results of equivalent circuit model with numerical results to validate the model.

The paper is organized as follows: Section II includes the design and configuration of the three metamaterial structures and its equivalent circuit models. In Section III, we present the numerical simulation results using HFSS and ADS software. Section VI includes conclusions.

R.Salhi,M. Labidi, and F. Choubani are with the Innov' COM Research Laboratory, Sup'Com, University of Carthage, Tunisia (e-mail: salhi.ridha89@gmail.com).

II. Equivalent Circuit Models

A. Split Ring Resonator (SRR)

Researchers have proved that an individual SRR can give the performances of SRRs arrays due to its periodicity [3].

We choose a set of geometry parameters of SRR presented in Fig. 1 as: D=1mm, S=1mm, W=0.5mm, L=6mm and the vertical size h=0.5mm For the SRR modeling, we use the equivalent circuit model as described in [4]. The geometry of an individual SRR with square form is shown in Fig. 1 and the equivalent circuit model is presented in Fig. 2.

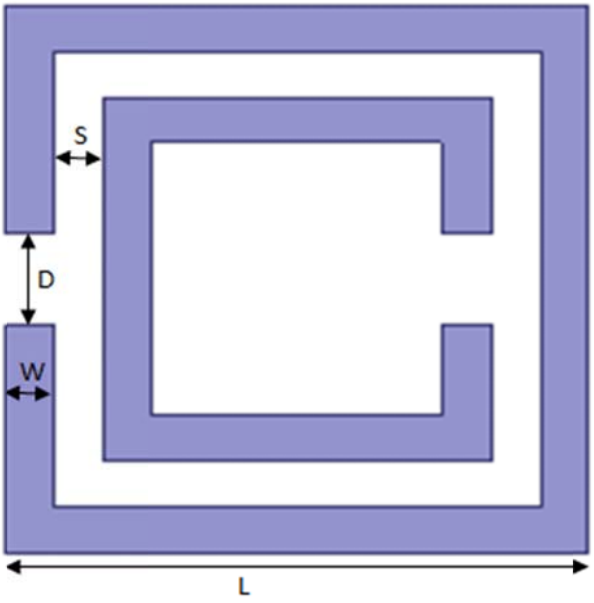

Fig. 1 The geometry configuration of a square SRR

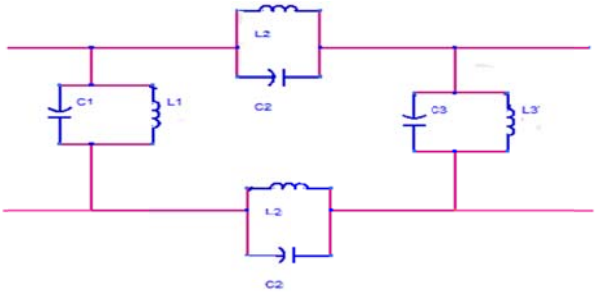

Fig. 2 The equivalent circuit model of SRR

The importance of the equivalent circuit model is to manipulate the structure with physical parameters. In literature, more precisely in [4], the expression of the inductances L1 and L3 are presented by (1):

$$L1 = L3 = \left(\frac{K\mu_0 n^2 L}{2\pi}\right)[\ln\left(\frac{2}{\rho}\right) + 0.5 + 0.178\rho + 0.0146\rho^2 + \frac{0.5(n-1)S^2}{(\rho n)^2} + \frac{0.178(n-1)S}{n} - \frac{1}{n}\ln\left(\frac{W+h}{W}\right)] \quad (1)$$

where

$$K = \frac{(2L-2S)-D}{(2L-2S)} \quad (2)$$

k is the integrality coefficient. Then, (3) gives the expression of L2:

$$L2 = \left(\frac{\mu_0 n^2 L}{2\pi}\right)[\ln\left(\frac{2}{\rho}\right) + 0.5 + 0.178\rho + 0.0146\rho^2 + \frac{0.5(n-1)S^2}{(\rho n)^2} + \frac{0.178(n-1)S}{n} - \frac{1}{n}\ln\left(\frac{W+h}{W}\right)] \quad (3)$$

where

$$\rho = \frac{nW + (n-1)S}{L} \quad (4)$$

Secondly, to calculate the capacitance of the equivalent model we will present 2 essential parts. The first part is the coupling capacitance between the outer and the inner ring.

$$Cc = (0.06 + 3.5 * 10^{-5}(r_{in} + r_{out})) \quad (5)$$

This coupling capacity Cc should be divided into 4 equal sub-parts named C_0 hence:

$$C_0 = \frac{1}{4}Cc \quad (6)$$

The second part is produced by an accumulate charge at the two splits.

$$Cin = (3\varepsilon_0 s / D) \quad (7)$$

$$Cout = (25\varepsilon_0 s / D) \quad (8)$$

where s is the parallel plan area. The capacitance C1, C2, and C3 can be determined by (9), (10), and (11):

$$C_1 = C_0 + Cout \quad (9)$$

$$C_2 = C_0 \quad (10)$$

$$C_3 = C_0 + Cin \quad (11)$$

B. High Impedance Surfaces

The High Impedance Surfaces (HIS) are structures with periodic pattern placed on a dielectric substrate and connected to the ground plane through metalized holes; they exhibit high impedance in a frequency band. The HIS were introduced by D. Sievenpiper [5], [6] in order to suppress the wave patch antenna surface and increase their performances.

The high-impedance surfaces possess very advantageous electromagnetic properties, as they do not allow the propagation of electromagnetic waves along their surface for certain frequency bands. In other words, these structures exhibit a prohibited frequency band, for which the surface wave propagation is forbidden. The high impedance surfaces belong to the class of photonic band gap structures (BIP). In the HIS, an incident wave arriving on such a surface would be totally reflected.

Fig. 3 shows the layout of a unit cell HIS. It consists of a square rectangular patch connected to a ground plane through metalized vias. It possesses a single layer containing a periodic network of period $a = w2+g$. The via radius r is equal to 0.4 mm. The patch has a width $w2$ = 5 mm and the spacing between the rings is g =2.5mm.

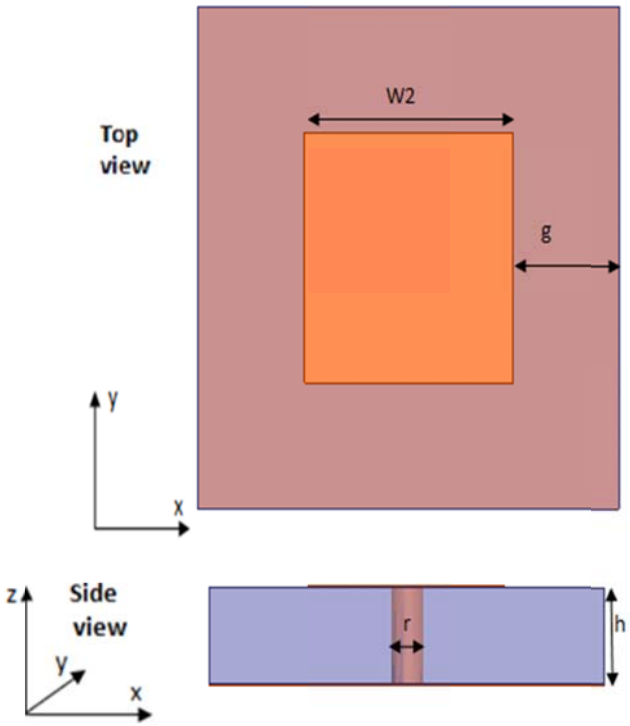

Fig. 3 The geometry configuration of HIS

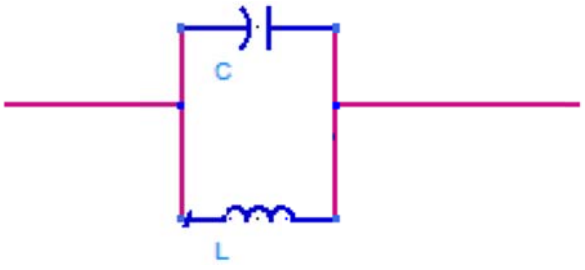

Fig. 4 The equivalent circuit model of HIS

The electrical equivalent circuit of the HIS unit cell is illustrated in Fig. 4. In this model, the inductance depends essentially on the dielectric substrate; it is given by (12). In this equation, h is the thickness of the substrate, μ_0 and μ_r are the permeability of vacuum, and the relative permeability of

the dielectric substrate [5] respectively.

$$L = \mu_0 \mu_r h \tag{12}$$

The equivalent capacitance is mainly due to the spacing between the metal hole. It is given by (13) where $\mathcal{E}_r$is the dielectric permittivity of the substrate [5].

$$C = \frac{b\varepsilon_0(1+\varepsilon_r)}{\pi} a\cosh\left(\frac{a}{g}\right) \tag{13}$$

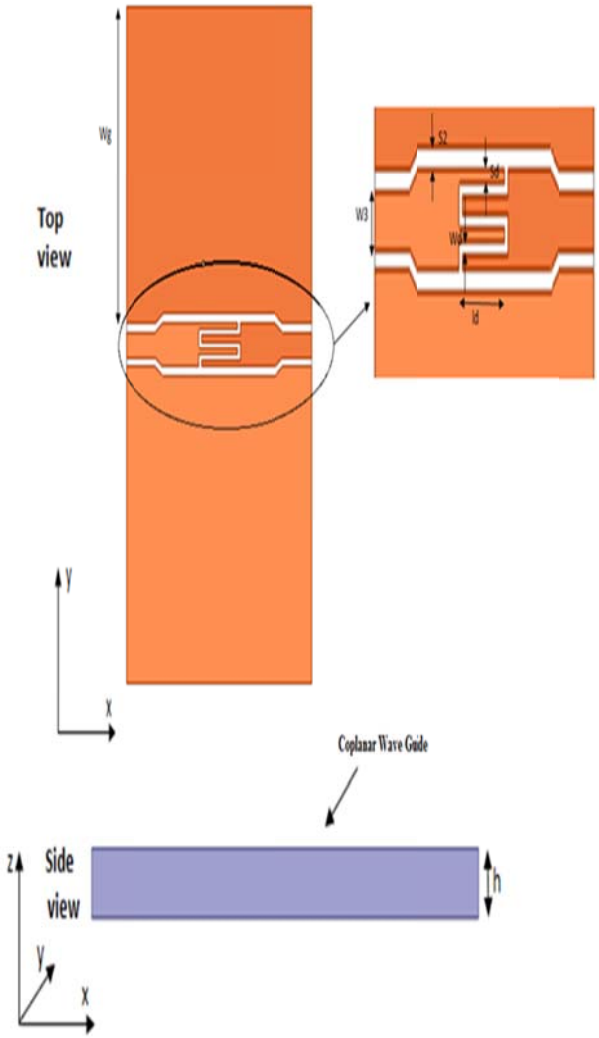

Fig. 5 The geometry configuration of IDC

Fig. 6 The equivalent circuit model of CPW

C. Coplanar Wave Guide

The coplanar transmission line also called Coplanar Wave Guide and denoted as CPW consists of three metal strips placed on the same plane at a constant distance of the dielectric substrate. The center conductor carries the microwave signal. The two lateral strips serving as ground planes and signal are separated by coplanar slots. In this section, we use the concept of CPW to design a special CPW called IDC (Interdigital capacity). Fig. 5 shows the geometry configuration of the IDC on a dielectric substrate (alumina) where *W3* represents the width of the center conductor, *S2* is the width of the coplanar slot *Wg* is the width of the two ground planes, *h* is the thickness of substrate and *t* is the thickness of the metallic conductors. Indeed, the values of these parameters are $w = 4wd + 3sd$, $S2$=0.3mm, Wg= 3w3,sd = wd=0.2mm and ld=3.1mm. Where wd represents finger width, ld represents finger length and sd represents spacing between the fingers. Our IDC is performed on a substrate of alumina (Al2O3) with 0,635mm thickness, a permittivity $\mathcal{E}_r$=9,2 and a loss tangent measured at 9,8 GHz of $6{:}10^{-4}$.

1) Calculation of the Capacitance

In the literature, there are several methods to extract the value of the interdigital capacity. In this study, we use the approach presented in [7]. The capacity expression is:

$$C_s = (\varepsilon_r + 1) l_d ((n-3)A1 + A2) \tag{14}$$

The coefficients *A1* and *A2* take into account the effects of the substrate thickness.

$$A1 = 4.409\tanh\left[0.55\left(\frac{h}{w}\right)^{0.45} 10^{-6}\right] \ (\mathrm{pF}/\mu\mathrm{m}) \tag{15}$$

$$A2 = 9.92\tanh\left[0.52\left(\frac{h}{w}\right)^{0.5} 10^{-6}\right] \ (\mathrm{pF}/\mu\mathrm{m}) \tag{16}$$

2) Calculation of Parasitic Capacitances

Parasitic capacitances *Cp* model the capacitance between the IDC and ground planes.

$$C_p = C_{acpw} l_d \tag{17}$$

In [8], the author proposes an approximate expression noting that the outer finger and the ground plane near him is a asymmetric coplanar line (ACPW) with a single ground plane. It has an asymmetric CPW signal line width *Wdeff* and a slit width *S2*. Such a structure has been studied in [9], [10], and capacitance per unit length is given by:

$$C_{acpw} = 2\varepsilon_0\left(\frac{K(k5')}{K(k5)}\right) + \varepsilon_0(\varepsilon_r - 1)\left(\frac{K(k6)}{K(k6')}\right) \tag{18}$$

$$k1 = \sqrt{\frac{w_{deff}}{w_{deff} + s}} \tag{19}$$

$$k_2 = \sqrt{\frac{e^{\frac{\pi w_{deff}}{h}} - 1}{e^{\frac{\pi (w_{deff}+s)}{h}} - 1}}) \quad (20)$$

$$k_i' = \sqrt{1 - k_i^2} \quad (21)$$

where K is the complete elliptic integral of the first type.

Taking into account the thickness of the metallization in the calculation, therefore we pass a finger width Wd to an effective width W_{deff} according to:

$$w_{eff} = w_d + \frac{t}{\pi}\left[1 + \ln\left(\frac{4\pi w_d}{t}\right)\right] \quad (22)$$

3) Calculation of the Parasitic Inductance

The inductance Ls is the parasitic inductance of interdigital capacity, it is determined as follows: Assuming that the magnetic field lines around each finger have a contribution inconsiderable compared to the magnetic field created around the entire capacity, this hypothesis is valid if $W_{eff}/h << 1$.

$$L_s = Z_c \sqrt{\frac{\varepsilon_{eff}}{c_0}} l_d \quad (23)$$

$$Zc = \frac{30\pi}{\sqrt{\varepsilon_{eff}}} \frac{K(k_3')}{K(k_3)} \quad (24)$$

$$k3 = \frac{w}{(w + 2s)} \quad (25)$$

$$k4 = \frac{\sinh\frac{\pi w}{2h}}{\sinh\frac{\pi(w+2s)}{2h}} \quad (26)$$

$$\varepsilon_{eff} = 1 + \left(\frac{\varepsilon_r - 1}{2}\right)\frac{K(k4)}{K(k_4')}\frac{K(k_3')}{K(k3)} \quad (27)$$

Indeed, Z_c and $\mathcal{E}_{eff}$ represent the characteristic impedance and the effective permittivity of the coplanar line respectively. They are calculated based on the geometric parameters of the coplanar line. Finally, c_0 is the speed of light in vacuum.

III. Numerical Simulation and Discussion

A. Split Ring Resonator

First, we use HFSS software to predict the resonance frequencies of SRR, and ADS is used to present the simulation results of its equivalent circuit model. Then the transmissions coefficients are shown in Fig. 7, these curves show that SRR and its equivalent model have three resonant frequencies respectively. We notice that S21 is less than -35dB at frequencies 6GHz, 16.8GHz and 27.8GHz. We note that S21 is less than -35dB at frequencies 6GHz, 16.81GHz and 27.11GHz, but in [5], S21 is less to - 35dB at frequencies 6GHz, 15.5GHz and 26.5GHz.

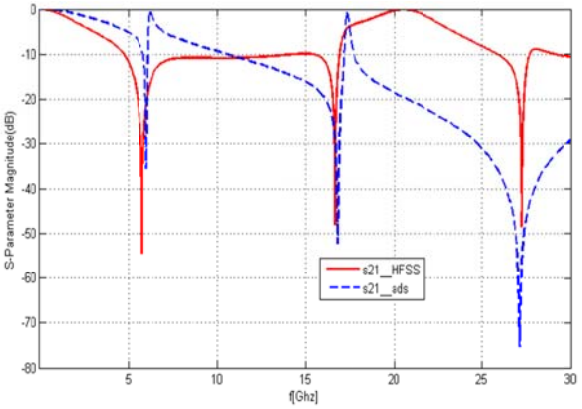

Fig. 7 The transmission coefficients of the SRR

B. High Impedance Surfaces

In this section, we present the results of transmission coefficient obtained from different demonstrators. We then seek to validate our simulation results by a circuit simulation of the equivalent HIS model. Fig. 8 illustrates the differences between the result of equivalent circuit model with numerical results and the simulation on the transmission and reflection parameter. Taking as a criterion of S21 should be less than -10 dB to define the frequency range where HIS is operate, it is from 1.23 GHz to 1.274 GHz with a resonance peak at 1.252 GHz.

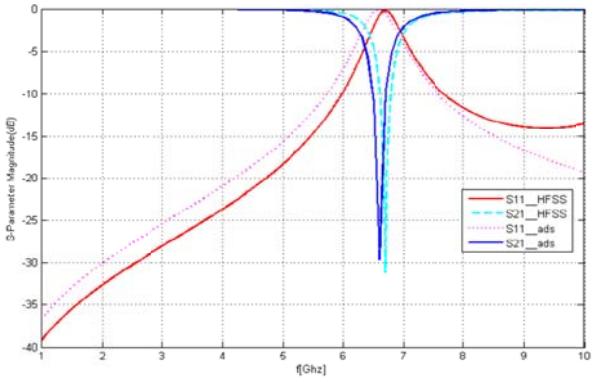

Fig. 8 The transmission and reflection coefficients of the HIS

C. Coplanar Wave Guide

Fig. 9 shows the scattering parameters of the model circuit and the electromagnetic simulation. There are good agreements between the results even if there are small differences between curves. The equivalent circuit model makes it possible to correctly describe the CPW to the frequency of 8.5 GHz.

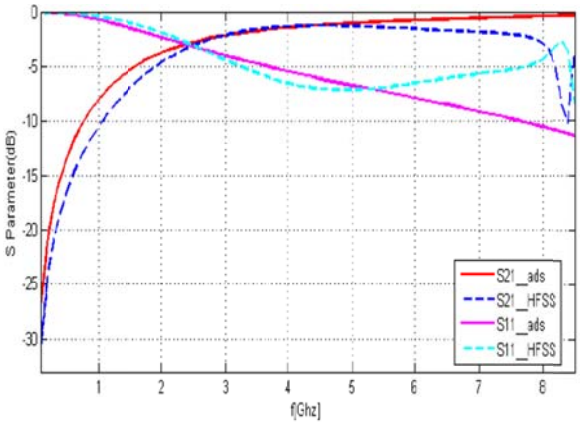

Fig. 9 The transmission and reflection coefficients of the CPW

IV. Conclusion

The modeling of structures in metamaterials is very important to properly interpret their physical behavior. We presented in this paper the modeling of three different structures in metamaterials that are SRR, SHI, and CPW. Then we compared the simulation results obtained by an equivalent circuit models with numerical simulation results to valid the models. This step is very important prior the extraction of effective electromagnetic parameters and the design of RF device.

References

[1] K. Buell, H.Mosallaei, and K. Sarabandi, "A substrate for small patch antennas providing tunable miniaturization factors," Microwave Theory and Techniques, IEEE Transactions on, vol. 54, no. 1, pp. 135–146, 2006.

[2] P. Talbot, A. Chevalier, and P. Queffelec, "Méthode de caractérisationélectromagnétique large bande des matériaux sous contraintemécaniqueoumagnétique," in 11émes Journées de Caractérisation Micro-ondeset Matériaux, 2010, p. 345.

[3] R.W. Ziolkowski, "Design, fabrication, and testing of double negative metamaterials," Antennas and Propagation, IEEE Transactions on, vol. 51, no. 7, pp. 1516–1529, 2003.

[4] M. Wu, F. Meng, Q. Wu, J. Wu, and L. Li, "A compact equivalent circuit model for the srr structure in metamaterials," in Microwave Conference Proceedings, 2005. APMC 2005. Asia-Pacific Conference Proceedings, vol. 1. IEEE, 2005, pp. 4–pp.

[5] D. Sievenpiper, L. Zhang, R. F. Broas, N. G. Alexopolous, and E. Yablonovitch, "High-impedance electromagnetic surfaces with a forbidden frequency band," Microwave Theory and Techniques, IEEE Transactions on, vol. 47, no. 11, pp. 2059–2074, 1999.

[6] L. Zhou, H. Li, Y. Qin, Z. Wei, and C. Chan, "Directive emissions from sub wave length metamaterial based cavities," Applied Physics Letters, vol. 86, no. 10, p. 101101, 2005.

[7] G. D. Alley, "Interdigital capacitors and their application to lumped-element microwave integrated circuits," Microwave Theory and Techniques, IEEE Transactions on, vol. 18, no. 12, pp. 1028–1033, 1970.

[8] A. Zermane, "Contribution `a l'étude et la faisabilité de micro-résonateursen structure planaire," Ph.D. dissertation, Université Jean Monnet-Saint-Etienne; Université de Constantine (Algérie), 2011.

[9] R. N. Simons, Coplanar waveguide circuits, components, and systems. John Wiley & Sons, 2004, vol. 165.

[10] G. Ghione, "A cad-oriented analytical model for the losses of general asymmetric coplanar lines in hybrid and monolithic mics," Microwave Theory and Techniques, IEEE Transactions on, vol. 41, no. 9, pp. 1499–1510, 1993.